Surface Modification Approach to TiO_2 Nanofluids with High Particle Concentration, Low Viscosity, and Electrochemical Activity
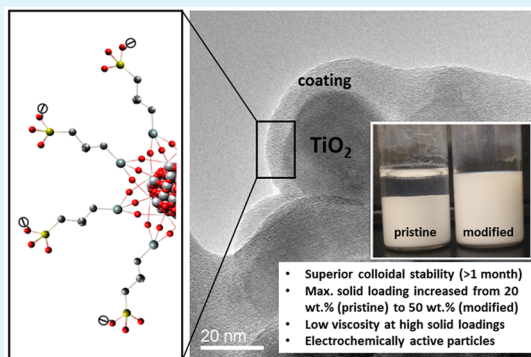
Sujat Sen,[*,†] Vijay Govindarajan,[†] Christopher J. Pelliccione,[†] Jie Wang,[‡] Dean J. Miller,[‡] and Elena V. Timofeeva[†]

[†]Energy Systems Division and [‡]Electron Microscopy Center - Center for Nanoscale Materials, Argonne National Laboratory, Lemont, Illinois 60439, United States

S *Supporting Information*

ABSTRACT: This study presents a new approach to the formulation of functional nanofluids with high solid loading and low viscosity while retaining the surface activity of nanoparticles, in particular, their electrochemical response. The proposed methodology can be applied to a variety of functional nanomaterials and enables exploration of nanofluids as a medium for industrial applications beyond heat transfer fluids, taking advantage of both liquid behavior and functionality of dispersed nanoparticles. The highest particle concentration achievable with pristine 25 nm titania (TiO_2) nanoparticles in aqueous electrolytes (pH 11) is 20 wt %, which is limited by particle aggregation and high viscosity. We have developed a scalable one-step surface modification procedure for functionalizing those TiO_2 nanoparticles with a monolayer coverage of propyl sulfonate groups, which provides steric and charge-based separation of particles in suspension. Stable nanofluids with TiO_2 loadings up to 50 wt % and low viscosity are successfully prepared from surface-modified TiO_2 nanoparticles in the same electrolytes. Viscosity and thermal conductivity of the resulting nanofluids are evaluated and compared to nanofluids prepared from pristine nanoparticles. Furthermore, it is demonstrated that the surface-modified titania nanoparticles retain more than 78% of their electrochemical response as compared to that of the pristine material. Potential applications of the proposed nanofluids include, but are not limited to, electrochemical energy storage and catalysis, including photo- and electrocatalysis.

KEYWORDS: nanofluids, anatase, low viscosity, colloidal stability, surface modification, thermal conductivity, electrochemical activity, nanoelectrofuel

- Superior colloidal stability (>1 month)
- Max. solid loading increased from 20 wt.% (pristine) to 50 wt.% (modified)
- Low viscosity at high solid loadings
- Electrochemically active particles

INTRODUCTION

Nanofluids are liquids that are engineered by stably dispersing functional nanomaterials in base fluids.[1,2] They have been historically investigated for their superior thermal properties, such as thermal conductivity and heat transfer, and typically considered for use in industrial and automotive cooling applications.[1−4] More recently, suspensions of functional nanomaterials have been investigated as media for chemical reactions,[5] thermal storage media,[6] solar harvesting applications,[7] electrochemical energy storage,[8] and in biomedicine and food.[1,2] A variety of nanoparticle materials in suspensions have been studied, including ceramics (titania,[9−11] alumina,[4,12,13] silica,[14] silicon carbide,[15] Fe_2O_3,[16] etc.), metals (silver,[17] copper,[18] tin,[6] iron,[19] etc.) and different forms of carbon[20] (graphite, graphene, carbon black, carbon nanotubes, etc.). A variety of base fluids have been tested for nanofluids, including water, alcohols, glycols, oils, and their mixtures. Complex behaviors exhibited by nanofluids have resulted in multiple theories attempting to explain the experimental viscosity and thermal conductivity enhancements.[4,21,22] However, no universal theory has been proposed that explains the behavior of the whole family of nanofluids. Discrepancies between the proposed theories and the experimental results are related to the multivariability of nanofluid systems with more than a dozen parameters that need to be controlled for accurate comparisons of different nanofluids. The systems engineering approach for nanofluid formulations[23] provides deeper insight into correlations within nanofluids and allows prioritizing some nanofluid parameters (particle concentration, material, size, etc.) to achieve the desired combination of properties, such as low viscosity and/or high thermal conductivity or other properties.

In this work, we utilize elements of system's engineering approach and focus on the development of nanofluids with the highest possible loading of titania (TiO_2) nanoparticles in aqueous electrolytes, which are of interest as new media for electrochemical energy storage and photo- and electrocatalysis. The target properties of such nanofluids are high colloidal stability, low viscosity, and high surface activity of the suspended nanoparticles. Titania nanoparticles were selected as a case study for this task, as they are currently used in a variety of applications

(e.g., solid photocatalyst[24] and solid battery anode material[25]) and also have a low cost and biocompatible nature.

Viscosity of nanofluids is a very important property for all applications that rely on fluid flow and pumping. A significant increase in viscosity of nanofluids over their base fluids is highly undesirable because any advancement in functional properties (e.g., heat transfer or catalytic efficiency) could be nullified by increased pumping power penalties. General trends observed in nanofluids indicate that viscosity increases with an increase in the particle concentration. For the same particle type and concentration, nanofluids in more viscous base fluids show smaller relative increases than in less viscous base fluids. Viscosity is typically higher in suspensions with smaller particles if all other nanofluid parameters are the same and particle agglomeration is minimized.[15,26] This behavior is related to the presence of the boundary layers between nanoparticles and the liquid, which are negligible in suspensions of micron-sized particles but contribute significantly to fluid properties at nanoscale particle sizes. Conversely, the use of larger particles to minimize viscosity has a drawback, such as potential colloidal instability of the resulting suspensions. Smaller nanoscale particles have higher kinetic energy (Brownian motion) and lower gravity force acting on it, resulting in inherently slower settling times. Nanoparticle shapes also affect the viscosity of suspensions with elongated nanoparticles, showing higher viscosity than spherical particles at the same volume concentrations.[12]

Interactions between nanoparticles affects viscosity of nanofluids through particle agglomeration phenomena. Depending on the particle concentration and the strength of particle–particle interactions, a dispersion/agglomeration equilibrium is established in the particle suspension. Extended agglomerates can provide increased thermal conductivity,[27] but agglomeration and clustering of nanoparticles result in a significant viscosity increase as the fluid microstructure from agglomeration provides resistance to fluid flow. Additionally, agglomeration causes faster settling of suspensions.[28,29] The agglomeration state of particles in suspensions can be influenced by pH, ionic strength, surfactant, and other additives[12,30] by either creating steric insulation (prevention of van der Waals interactions between particles) or by increasing the electrostatic repulsion (controlling surface charges at nanoparticles, i.e., increasing zeta potential).

To date, achieving a high concentration of nanomaterials in suspension without dramatic increases in viscosity remains the main challenge in nanofluid engineering. Most studies on nanofluids for heat transfer have only reported on nanoparticle loadings between 0.1 and 10 wt % because of huge viscosity increases at higher concentrations that deemed the fluid impractical. Use of surfactants to improve colloidal stability[31,32] and viscosity of suspensions has been successful, but typically has adverse effects on other useful properties, such as thermal conductivity of the suspension.[33] This is attributed to the low thermal conductivity of surfactants that wrap around the particles and act as a thermal resistance layer. Additionally, the use of surfactants interferes with functional properties of the nanoparticle surface, preventing electrochemical and catalytic processes at the solid–liquid interface.

Nanofluids of rutile or anatase TiO_2 in water have been previously investigated by several groups as prospective heat transfer fluids.[9,10,13,33−42] Aqueous titania nanofluids have been typically reported at concentrations below 10 wt %.[35,43−47] Utomo et al.[13] studied the viscosity of aqueous dispersions of titania (20−30 nm) at concentrations up to 6 wt % (∼1.5 vol %). Relative viscosity increases of up to 300% were reported for a 6

wt % dispersion. Dispersants such as CTAB,[48] SDS,[36] acetic acid,[49] or Span 80[45,49] have been used to obtain high concentrations of nanoparticles in suspensions. Fedele et al.[49] studied aqueous titania nanofluids with up to 35 wt % solids with acetic acid as the dispersant (up to 5 wt %, pH 3). The resulting nanofluid had a thermal conductivity enhancement of 21% and 300% increase in viscosity.

Tseng et al.[50] reported the rheological properties of anatase nanofluids with 16−34 wt % (5−12 vol %) loading of 7−20 nm particles in deionized water at neutral pH. Viscosities at room temperature were up to 1200 cP for the highest solid loading. Higher particle loadings up to 75 wt % were typically achieved for submicron particles. Chandler[51] reports on the viscosity of aqueous suspensions with 0.72 μm anatase particles. At loadings of 61−70 wt % (30−38 vol %), viscosities ranged from 10 to 100 cP at room temperature. Gomez-Merino et al.[52] reported the rheological properties of a 0.15 μm anatase particle suspension in aqueous 10 μM KCl solution at pH 7. Shear-thinning behavior was observed for fluids with a volume fraction between 48 and 75 wt % (20−45 vol %). In the range of shear rates between 0.0032 and 2032 s^{-1} the viscosities of the fluids with 48 wt % (20 vol %) of solids ranged from 2 to 20 cP, and for suspensions with 75 wt % (45 vol %) in the same shear rate range, viscosities varied from 150 to 40000 cP. Dynamic light scattering (DLS) results confirmed the formation of extended agglomerates at rest, which are the reason for observed shear thinning behavior. At high shear rates, agglomerates either align or partially break down to achieve a lower agglomeration state, resulting in lower viscosity of suspensions. Yang et al.[53] also reported the shear-thinning behavior of aqueous suspensions with 0.24 μm anatase particles with loading varying between 16 and 74 wt % (5−43 vol %). At 54.5 wt % (24 vol %) particle loading and neutral pH, extremely high viscosities were reported ranging from 200 to 50000 cP at high (1000 s^{-1}) and low (0.1 s^{-1}) shear rates, respectively. For the highest loadings of 74 wt % (43 vol %), the range of viscosities was between 10^4 and 10^8 cP for the same range of shear rates. Furthermore, they investigated the effect of pH from 1.2 to 9.1 on the rheology of a 54.5 wt % (24 vol %) anatase suspension. The suspension with pH 9.1 had the least shear rate dependence, observing a variation between 20 cP and 200 cP and for the corresponding high and low shear rates. The highest viscosity was observed between pH 5 and 6.5, showing variation between 8×10^5 cP and 200 cP for low and high shear rates. This result is consistent with established point of zero particle charge (isoelectric point) that falls in the pH 5−6 range for anatase titania. It should be noted here that none of these studies report any information on the long-term colloidal stability of the prepared suspensions.

Furthermore, all studies that achieve acceptable levels of viscosity typically use significant amounts (>5 wt %) of surfactant additives. Because these additives are electrochemically inactive, they are likely to diminish the electrochemical and catalytic activity of the nanoparticle material targeted in this study. Thus, in this study, we develop an alternative approach to control the viscosity and colloidal stability of suspensions, namely, the surface modification of the nanoparticles with anchored functional groups.[54]

Surface grafting of polymeric or functional moieties onto nanoparticles has been previously explored to moderate nanopowder properties.[29,54−57] Polymeric coatings often result in thick layers on the surface adding up to 25−30 wt % to the nanoparticle material. This reduces the fraction of active material in suspension at the same solid particle loading and likely isolates

the surface of the particle from direct contact with the electrolyte, thereby affecting surface activity. For the purpose of this study, we selected an approach that uses small functional groups for surface modification to minimize the weight fraction of the grafting agent. A small organic molecule with sulfonate or sulfate groups anchored to the surface of a nanoparticle can provide both steric and charge-based separation in polar solvents or electrolytes while only partially blocking active surface sites. This approach has been previously used to provide better acidic properties and hydrophilic nature to titania nanoparticles intended for use as heterogeneous catalysts.[58−60] Atghia et al.[58,59] reported a two-step procedure using a thiol-functionalized silane to modify the titania surface. The thiol was subsequently oxidized to a sulfonate group. Rahmani et al.[60] also reported an approach to synthesize sulfonated titania by a direct reaction with chlorosulfonic acid, which is a highly corrosive reagent. The resulting sulfonated titania was used as a solid-state heterogeneous catalyst for a variety of organic reactions. Sulfated titania has also been prepared by direct treatment with sulfuric acid and ammonium sulfate.[61−64] In all cases described above, surface-modified titania was found to be recyclable and highly chemoselective with high reaction rates and excellent yields.

In this study, we target the development of a simple process for coating titania nanoparticles that can be scaled-up for industrial nanofluid production while providing the requisite colloidal stability, low viscosity, and surface activity while minimizing the weight contribution of the surface grafting agent. Using pristine and surface-grafted titania nanoparticles, we further prepare nanofluids in alkaline electrolyte solutions (pH 11) at the highest possible concentrations. The resulting nanofluids are characterized with respect to fluid properties, such as dispersion stability, viscosity, thermal conductivity, as well as electrochemical activity of pristine and modified nanoparticles as solid-casted electrodes.

■ EXPERIMENTAL SECTION

Materials and Characterization Techniques. Commercially available anatase titania nanopowders with average particle sizes of 25 nm (Sigma-Aldrich, BET) were used in this study. The morphology of the nanoparticles was examined using scanning electron microscopy (SEM, Hitachi S-4700) and analytical transmission electron microscope (TEM, FEI Tecnai F20ST). Samples for imaging were prepared by drop-casting highly dilute suspensions of the nanoparticles in ethanol onto a silicon wafer (SEM) or carbon-laced copper grid (TEM). Crystalline structure was confirmed through X-ray powder diffraction measurements (XRD, Bruker D2 diffractometer). Thermogravimetric analysis (TGA, SDT Q-600, TA Instruments) of TiO_2 nanoparticles before and after surface modification was conducted to quantify the amount of grafted material. In a typical test, a 10−15 mg sample was heated from 30 to 800 °C at 10 °C/min under N_2 flow (100 mL/min). Loss in mass of the sample during such a test was ascribed to the loss of water and grafting moiety.

Surface Modification of Titania Nanoparticles. Three grams of pristine titania nanoparticles (TiO_2) were mixed with 25 mL of deionized water. At the same time, 4 g of 40 wt % 3-(trihydroxysilyl)-1-propanesulfonic acid (SIT, Gelest) was diluted in 20 mL of deionized water. The titania suspension was slowly added to the SIT solution while stirring vigorously in a round-bottom flask. To this mixture was added 1 M solution of sodium hydroxide (NaOH, Fisher Scientific) dropwise until the mixture reached pH 5. The reaction mixture was then heated to 80 °C and stirred vigorously for 24 h under the inert gas purge (Ar). The resulting sulfonated titania particles (TiO_2−S) were then washed profusely with deionized water and ethanol, isolated by centrifuging, and dried under vacuum.

Preparation of Nanofluids. Mixed aqueous alkaline solution containing both 30 mM KOH and 10 mM LiOH in deionized (DI) water (net hydroxide concentration of 40 mM) was chosen as the base fluid electrolyte in preparation of all nanofluids in this study and representative of salts and additives that are typically used in industrial processes and in alkaline battery electrolytes.[25] A pH of ~11 in the resulting nanofluids provides for the maximum zeta potential at which colloidal stability of titania particles can be achieved[34] (electrostatic stabilization). Electrical conductivity of this electrolyte was measured (EC Tester 11plus, Oakton Instruments) to be 2.81 mS. In a general nanofluid preparation procedure, the requisite amount of dry nanopowder was added to the base fluid and mixed extensively to achieve a homogeneous suspension. Nanoparticle concentrations are reported in weight percent, which is the fraction of nanoparticle mass present in the total mass of the nanofluid, e.g., 30 g of solid and 70 g of base fluid make up 100 g of a 30 wt % nanofluid. Conversion of weight percent to volume percent for aqueous TiO_2 suspensions is presented in Supporting Information Figure S1. Magnetic stirring was used for mixing the nanoparticle and the base fluid for at least 24 h. The suspensions were then sonicated (ultrasonic bath, 37 kHz) for 4−6 h. Prior to any testing, nanofluids were reagitated for at least 1 h with sonication. pH was measured after mixing, and if necessary, it was adjusted to pH 11 with 3 M KOH solution (typically 1−2 drops). In this pH adjustment procedure, the added amount of KOH (<0.06 mL added to 100 mL of total volume) has a negligible effect on the total nanofluid volume (0.06%) and changes the concentration of hydroxide (<5%), and hence, the initial values of the nanoparticle and electrolyte concentrations are still accurate. Initially, nanofluids were prepared from unmodified "pristine" TiO_2 nanoparticles of different sizes with particle loadings of 10 and 20 wt % (sections 1.2 and 1.3 in the Supporting Information). Viscosities of those suspensions were evaluated. At particle concentrations higher than 20 wt % of pristine TiO_2, particles resulted in extremely viscous suspensions with a pastelike consistency. Further, the surface modification of 25 nm titania nanoparticles was conducted, and nanofluids were prepared from the surface-modified nanopowders using the same preparation protocol.

Measurements of Nanofluid Properties. The nanofluid's thermal conductivity was measured using a thermal property analyzer based on the transient hot wire method (KD2pro, Decagon Devices, Inc.) with a KS-1 probe with accuracy ±0.01 W/mK for conductivities between 0.2 and 2 W/mK. The effective thermal conductivity values reported for nanofluids and the base fluid represent an average value for 100 measurements taken at room temperature (21 ± 0.5 °C) with 15 min intervals. The dynamic viscosity of the nanofluids was measured using a rotational-type viscometer (Brookfield DV-II+, Brookfield Instruments) with the SC4-18 spindle with accuracy ±1% of the maximum viscosity range at given rotational speed. Calibration curves at different temperatures along with literature viscosity values[65] are presented in Figure 6a for the ethylene glycol−water mixture and in Figure S4b for pure ethylene glycol. Reported experimental viscosity for nanofluids correspond to an average of 25 consecutive readings. The viscosity of nanofluids was measured in the temperature range between 15 to 55 °C ± 0.2 °C at a shear rate of 264 s^{-1}. Dynamic light scattering (DLS) measurements (Particle size analyzer, ZetaPlus, Brookhaven Instruments Corp.) were used to evaluate the agglomeration state of nanoparticles in electrolyte. Dilute (<0.01 wt %) suspensions of pristine and sulfonated nanoparticles in the base fluid electrolyte, ensuring pH 11, and ionic strength were examined. Zeta potential was measured using the electrophoretic light scattering (ELS) function in dilute (<0.01 wt %) 1.3 mM aqueous KOH solution, ensuring pH 10 and conductivity of ~400 μS.

Electrochemical Testing. Electrochemical properties of pristine and surface-modified titania were evaluated in the form of solid-casted electrodes. Mixed together were 0.4 g of active nanomaterial (pristine or sulfonated titania), 50 mg of polyvinyldifluoride binder (PVDF), and 50 mg of acetylene black (80:10:10 ratio). The dry powder was thoroughly mixed using a vortex mixer. A few drops of N-methyl-2-pyrrolidone (NMP) were added to make a paste, which was then sonicated, coated onto a titanium gauze, and dried in an oven (at 60 °C). Electrochemical testing was conducted (EZstat Pro potentiostat/galvanostat, Nuvant Systems Inc.) using this coated electrode as the working electrode, a graphite rod as counter electrode, and Hg/HgO reference electrode in

an aqueous solution of 4 M KOH/1.5 M LiOH. Cyclic voltammetry curves (CV) were measured at a scan rate of 5 mV/s between potential limits of −1.4 and −0.4 V relative to Hg/HgO.

■ RESULTS AND DISCUSSION

Characterization of Surface-Modified TiO₂−S Nanoparticles. Commercially available titania nanoparticles (anatase phase) were purchased in a variety of size ranges (from 5 to 100 nm). Titania nanoparticles with nominal sizes of 25 nm were selected for surface modification due to their sphericity and narrow particle size distribution (see sections 1.2−1.3 in the Supporting Information). The surface grafting procedure described in the Experimental Section resulted in titania powders with chemically modified surfaces (TiO₂−S). Reaction of hydroxyl groups on the surface of titania with the grafting agent 3-(trihydroxysilyl)-1-propanesulfonic acid (SIT) forming (Ti-O)₃-Si-(CH₂)₃-SO₃⁻ bonds renders the surface of the titania nanoparticles with negatively charged sulfonate groups. The XRD spectra before and after the surface modification (Figure 1)
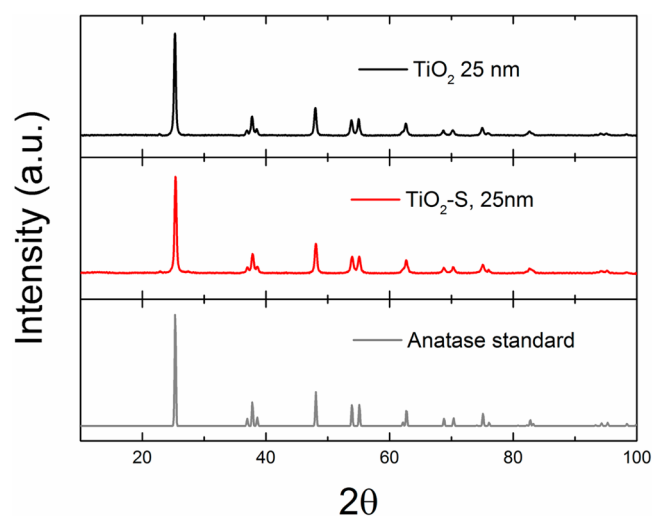

Figure 1. X-ray diffractograms (XRD) for pristine TiO₂ particles and titania with the grafted sulfonate groups (TiO₂−S) compared to the database standard for anatase TiO₂.

show the anatase phase for both pristine and modified titania,[66] also confirming that chemical modification did not affect the crystalline structure of nanoparticles. Slight peak broadening is observed in both cases, which is expected in nanosized particles. On the basis of the Scherrer equation, grain sizes were estimated from XRDs at 20 ± 2 nm for both samples.

SEM images of nanoparticles after surface modification clearly show the presence of an organic coating on the surface appearing as a charge accumulation halo around the particles (Figure 2b). Average particle sizes of ∼30 nm and spherical shapes remained unchanged after the surface modification. Surface-modified TiO₂−S particles tend to assemble into agglomerates on the surface of the silicon wafer (see SEM sample preparation); however, one can clearly see from SEM (Figure 2a and b) and TEM images (Figure 2c−f) that particles are separated from each other with a coating layer. TEM images clearly show amorphous coating on the surface of individual nanoparticles with an average thickness of ∼5 nm, varying from 2 to 10 nm.

Thermogravimetric analysis (TGA) of pristine and surface-modified samples are shown on Figure 3. In the temperature range between 25 and 100 °C, both TiO₂ and TiO₂−S samples

showed ∼0.5 wt % loss, which corresponds to the loss of physiosorbed water. Further heating to 800 °C resulted in additional loss of 0.5 wt % in the pristine titania sample, possibly due to loss of hydroxyl groups on the surface. The TiO₂−S sample exhibited an additional ∼2.5 wt % loss when heated to 800 °C, which is related to the degradation of the grafting moiety and loss of organic surface groups. The net loss of mass for the TiO₂−S sample is ∼3 wt %, which is significantly smaller than the ∼30 wt % reported in the literature for comparable surface grafting methods (Table 1).[58−60] TGA results indicate a relatively low grafting density of 0.15 mmol/g, suggesting that the surface modification procedure employed here minimizes self-condensation and other side reactions of the grafting agent. Furthermore, a simple calculation (see section 1.4 in the Supporting Information) of the expected monolayer coverage of the grafting moiety on the surface of 25 nm titania nanoparticles reveals that a 2% change in mass is expected for a densely packed monolayer, which is very close to the coverage observed experimentally. Because the objective of the study was to maximize the nanoparticle concentration in the nanofluid while minimizing any additives/grafting molecules, a low grafting density while achieving the desired colloidal and rheological targets was ideal for our application.

Table 1 briefly compares reported methods of sulfonation and sulfation to this study in terms of simplicity of the protocol, application, and amount of additive introduced. Use of corrosive reagents or multistep protocols makes the process hard to scale up and labor and cost intensive. The procedure employed in this study is one-step using relatively mild reagents available commercially and hence easily scalable.

Characterization of Nanofluids with TiO₂−S Particles. Colloidal stability is a key factor for the long-term performance of nanofluids in different applications and was evaluated as settling rate over time. Prior to the stability test, prepared nanofluids were reagitated through 1 h sonication and then left to rest. Photographs were taken as settling patterns developed (Figure 4).

Figure 4 shows that nanoparticles of pristine titania began to settle after a few hours at rest, whereas nanofluid with TiO₂−S had minimal sedimentation even after 1 month at rest, indicating significant improvement in dispersion stability due to the surface modification. The dynamic light scattering (DLS) technique was used to study the agglomeration state of nanoparticles within the nanofluids for both pristine and sulfonated nanoparticles (Figure 5). DLS measurements are limited to the particle concentrations that allow a level of transparency for the passage of light without multiple scattering events. This is typically possible in dilute suspensions (<0.01 wt %) as described in the Experimental Section and not possible to perform in concentrated suspensions. DLS results indicate the state of particle aggregation in a given base fluid and can be affected by pH and ionic strength. We used the same base fluid electrolytes to prepare samples for DLS, ensuring the same pH and ionic strength in dilute and concentrated suspensions. Number distribution spectra (Figure 5) show peaks at 623 and 30 nm for pristine TiO₂ and TiO₂−S particles, respectively, indicating that in the case of pristine nanoparticles, large agglomerates are present in the suspension, whereas in suspensions of surface-modified nanoparticles, good dispersion is achieved and individual particle sizes are maintained. Zeta potential measurements demonstrated values of −40 ± 2 mV for pristine TiO₂ and −60 ± 3 mV for sulfonated TiO₂−S particles at pH 10. The higher surface charge on TiO₂−S nanoparticles prevents particle agglomeration resulting in good
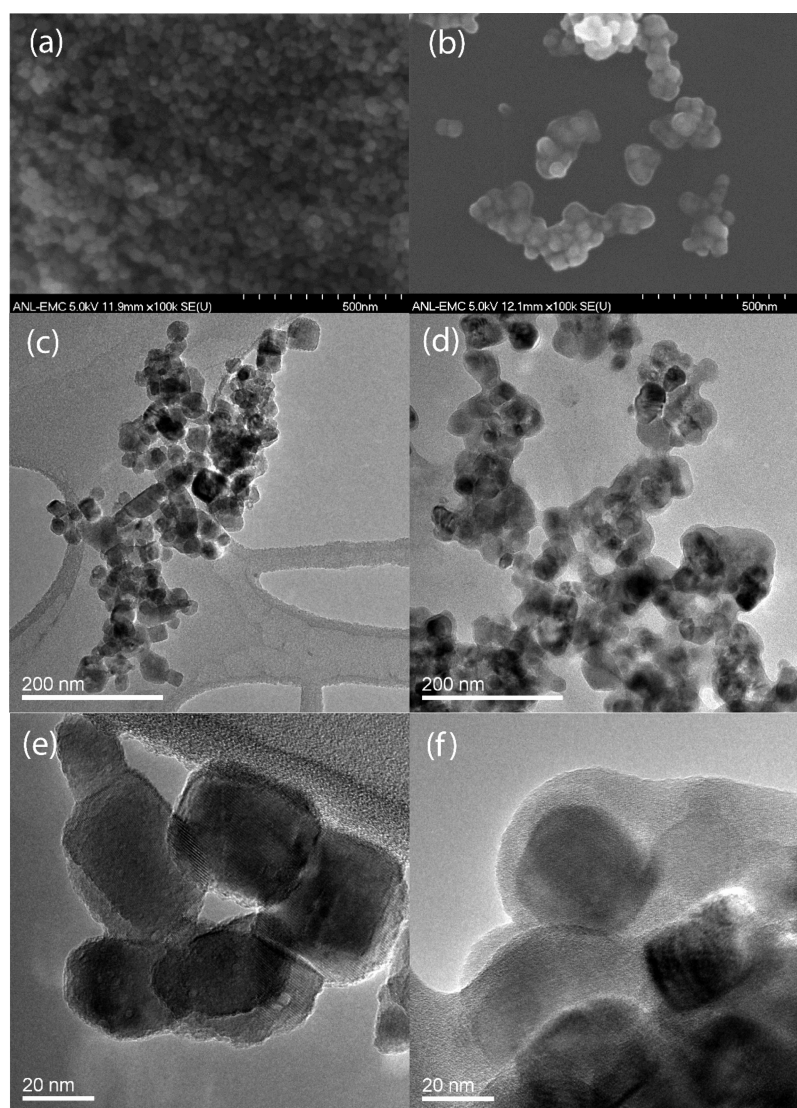
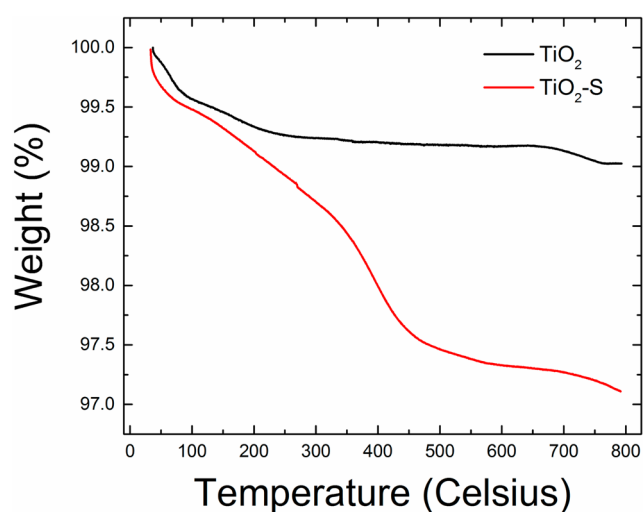**Figure 2.** Electron microscopy images of TiO_2 particles before (a, c, e) and after (b, d, f) surface modification (TiO_2−S).

Figure 3. TGA analysis of pristine (TiO_2) and sulfonated (TiO_2−S) nanoparticles.

particle dispersion and long-term colloidal stability. DLS and zeta potential results provide a baseline understanding of the

nanoparticles' ability to disperse in a particular liquid; however, other parameters, most notably the increase in solid loading of the nanofluid, can have additional effects on the state of particle agglomeration.

With TiO_2−S nanopowders, we were able to prepare a series of nanofluids with particle loadings up to 50 wt % with superior suspension stability. Figure 6a presents the viscosity as a function of temperature and different TiO_2−S particle loadings. At 25 °C, the highest viscosity of 4.33 cP was observed for the nanofluid with 50 wt % TiO_2−S loading, which is an ∼4-fold increase over that of the base fluid. This is in direct contrast to the 20 wt % suspension of pristine TiO_2 particles, which at the same temperature had viscosity exceeding 15 cP (see Figure S4). With increasing test temperatures, viscosities of the nanofluids decreased similar to the viscosity of the base fluid. Viscosities of the nanofluids with up to 50 wt % TiO_2 particle loadings were found to be shear independent and provide stable viscosity values over extended measurement times (see Figure S5), suggesting that the surface coating effectively prevents the formation of agglomerates. Attempts at preparing nanofluids with even higher solid loadings, i.e., 60 wt %, resulted in an unstable suspension with visible amounts of sediment forming during the measure-

Table 1. Comparison of the Current Work to Literature References for Reaction Conditions of Titania Powders Modified with Sulfate and Sulfonate Groups

ref	grafting agent	reaction conditions	weight fraction of grafting agent	notes and application
Atghia et al.[58,59]	3-mercaptopropyl trimethoxysilane	toluene, reflux, 24 h followed by peroxide treatment	~30 wt %	multistep protocol, used as solid state catalyst
Rahmani et al.[60]	chlorosulfonic acid	drop-wise addition over 1 h, ice bath	~20 wt %	highly corrosive reactant, used as solid state catalyst
Samantaray et al.[63]	ammonium sulfate	solid−solid kneading followed by slow heating to 773 K for 3 h	2.5−10 wt %	alkylation catalyst for fixed-bed reactor, photocatalysis
Samantaray et al.[63]	sulfuric acid	aqueous impregnation followed by calcination at 773 K for 3 h	2.5−10 wt %	alkylation catalyst for fixed-bed reactor, photocatalysis
this work	3-(trihydroxysilyl)-1-propanesulfonic acid	water, pH 5, 80 °C, 24 h	<3 wt %	mild reactant in a single step protocol, low viscosity nanofluids
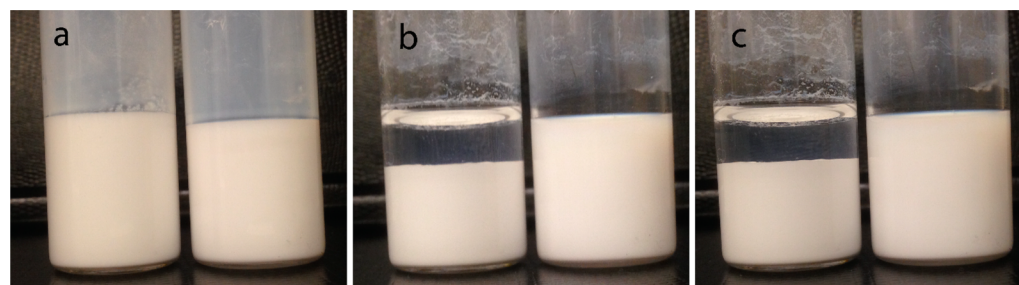
Figure 4. Settling tests for 10 wt % dispersion of pristine TiO_2 (left) and TiO_2−S (right) in 30 mM KOH and 10 mM LiOH over (a) 0 h, (b) 72 h, and (c) 1 month.
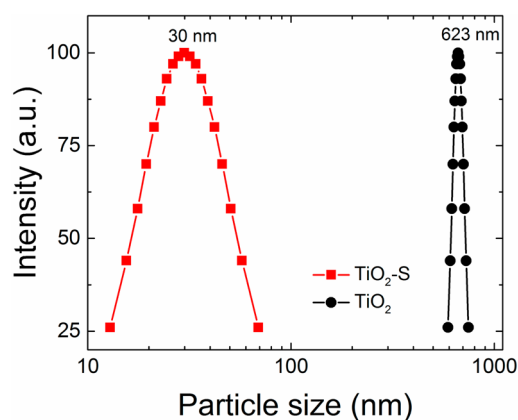
Figure 5. DLS results showing number log-normal particle size distributions for dilute TiO_2 and TiO_2−S nanofluids.

ment. Viscosity of the TiO_2−S nanofluids at 50 wt % is lower than most reported in the literature for nanoscale particle sizes. In particular, our nanofluids with 30 wt % (10 vol %, pH 11) solid loading have 2.50 cP viscosity relative to 50 cP of a 30 wt % (10 vol %, pH 11) nanofluid reported by Marchant et al.[67] Tseng et al.[50] reported a viscosity of 1200 cP for 34 wt % anatase nanofluids (particle size 7−20 nm, pH 7). It appears that it is easier to achieve lower viscosity suspensions with high particle loadings when larger particles are used, such as 0.15,[52] 0.24,[53] and 0.75 μm[51] anatase titania suspensions that have reported up to 75 wt % solid loading. However, in all these cases, viscosity had a strong shear-dependent behavior, and colloidal stability of such suspensions were not discussed.

Experimental viscosity of the TiO_2−S nanofluids at 25 °C were compared with the most common theoretical viscosity models (Figure 6b). The viscosity of TiO_2−S nanofluids appear to be linearly increasing with particle loading for suspensions with up to 40 wt % (15 vol %). At higher concentrations, the increase is

significantly steeper, indicating the onset of stronger particle−particle interactions. Classical Einstein−Batchelor model describes suspensions of noninteracting hard spheres[13]

$$\eta_{relative} = \frac{\eta_{nf}}{\eta_0} = 1 + 2.5\phi + 6.2\phi^2 \tag{1}$$

where $\eta_{relative}$ is the viscosity of the suspension (η_{nf}) relative to the base fluid (η_0), and ϕ is the volume fraction of solid particles in the fluid. The relative viscosity of TiO_2−S nanofluids is higher than predicted by the Einstein−Batchelor model, indicating particle interactions. The Krieger−Dougherty relationship is a semiempirical model that takes into account a "crowding effect" that exists in more concentrated suspensions leading to greater sensitivity to changes in particle concentration. It includes an additional parameter, ϕ_m, the maximum packing fraction. This is defined as the maximum volume of particles that can be added to a suspension before the system "jams up" and viscosity becomes infinite.[68]

$$\eta_{relative} = \frac{\eta_{nf}}{\eta_0} = \left(1 - \frac{\phi}{\phi_m}\right)^{-[\eta]\phi_m} \tag{2}$$

where $[\eta] = 2.5$ is the intrinsic viscosity.

Furthermore, the modified Krieger−Dougherty model adds another "effective aggregate" term, ϕ_{agg}, replacing the solid volume fraction (ϕ) term in eq 2 defined as[13]

$$\phi_{agg} = \phi\left(\frac{a_a}{a}\right)^{3-D_f} \tag{3}$$

where a_a is the radius of the aggregate (estimated from DLS measurements), a is the radius of the particle, and D_f is the fractal dimension of aggregates in the nanofluid with typical values between 1.6 and 2.5.[13] As one can see from Figure 6b, the best fitting model for our experimental results is the modified Krieger−Dougherty model with D_f = 1.6. The fit results in ϕ_m =
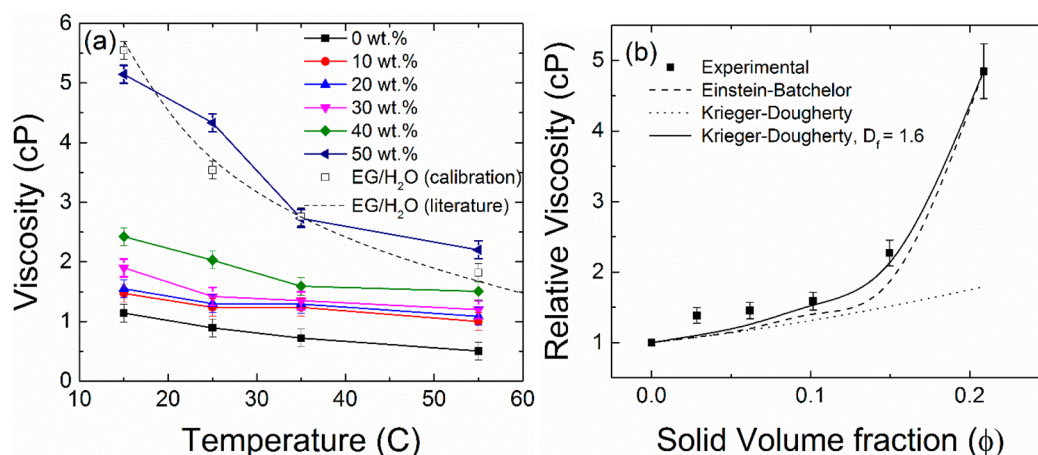
Figure 6. Dynamic viscosity measurements of (a) sulfonated TiO$_2$−S nanofluids at various temperatures and solid loadings; the calibration curve is a 0.25 mole fraction of ethylene glycol in water included as reference. (b) Relative viscosity of TiO$_2$−S nanofluids at 25 °C as a function of the solid volume fraction compared to predictions of theoretical viscosity models.

0.3, indicating that the maximum achievable concentration of solids in the system is 60 wt % (30 vol %). Fitting into the original Krieger−Dougherty model yielded a value of ϕ_m = 0.22. Hence, both models predict a maximum packing volume fraction of approximately 22−30 vol %. This is relatively close to the experimentally obtained 50 wt % (21 vol %) suspension, beyond which suspensions were found to be unstable. Similar fitting of experimental viscosity of nanofluids with pristine particles using the original Krieger−Dougherty model shows a maximum loading (ϕ_m) of 20 wt % (6 vol %) of pristine 25 nm TiO$_2$ particles. These results clearly show advantages of using surface grafted nanoparticles for preparing the suspensions with high solid loadings.

Thermal conductivities of nanofluids with pristine (TiO$_2$) and sulfonated (TiO$_2$−S) titania were measured to determine the effects of surface modification and high particle loading. Figure 7
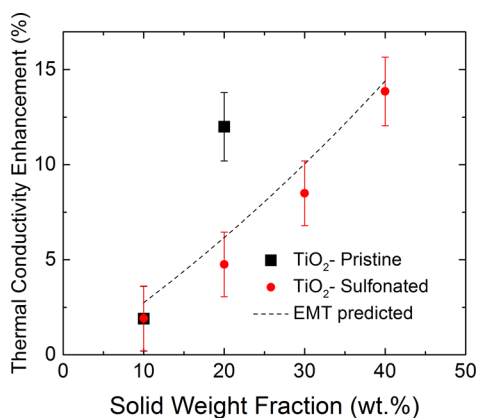

Figure 7. Enhancement in thermal conductivity at room temperature over the base fluid as a function of nanoparticle loading for TiO$_2$ and TiO$_2$−S; values predicted by effective medium theory (EMT) are included for comparison.

shows the results for both TiO$_2$ and TiO$_2$−S series as an enhancement in thermal conductivity with nanoparticle concentrations (relative to the base fluid values, measured as 0.579 Wm^{-1} K^{-1} at ambient room temperature).

Effective medium theory (EMT) is typically used for predicting the thermal conductivity of nanofluids with ceramic particles[69]

$$\frac{k_{nf}}{k_0} = 1 + \frac{3(k_p - k_0)\phi}{(k_p - 2k_0)} \tag{4}$$

where ϕ is the volume fraction of solid particles, k_{nf}, k_p, and k_0 are the thermal conductivities for the nanofluid, solid particles, and base fluid, respectively. Assuming a value of k_p = 1.4 Wm^{-1} K^{-1} for titania nanoparticles,[70] Figure 7 shows an EMT-based prediction for thermal conductivity enhancement at different weight fractions of titania particles. Experimental results for thermal conductivity of TiO$_2$−S nanofluids show values within the margin of error from those predicted by EMT, which linearly increases with particle loading. Nanofluids from pristine nanoparticles, however, show different behavior. At 10 wt % solid loading, the experimental thermal conductivity of nanofluids with pristine nanoparticles is the same as in the equivalent TiO$_2$−S system. As particle concentration is increased to 20 wt %, the experimental thermal conductivity is significantly higher than the 20 wt % TiO$_2$−S nanofluid or the EMT prediction. This result is most likely related to a high degree of nanoparticle agglomeration in nanofluids with pristine titania, which was also indicated by a dramatic viscosity increase in this nanofluid. Nanoparticle agglomerates provide extended paths for heat conduction, which are more efficient than thermal conduction through solid/liquid/solid paths.

For the nanofluids with particle concentrations below the aggregation threshold (e.g.,10 wt % in nanofluids with pristine TiO$_2$), it can be concluded that the surface modification does not have a significant effect on the thermal conductivity of suspensions as similar values were observed for both TiO$_2$ and TiO$_2$−S systems. At higher concentrations, surface groups on TiO$_2$−S nanofluids prevent particle agglomeration and therefore minimize agglomeration-based thermal conductivity enhancement mechanisms, maintaining thermal conductivity values close to the EMT prediction. Literature results on the thermal conductivity of TiO$_2$ nanofluids have significant variation with some researchers reporting >30% enhancements at 17 wt % (5 vol %) of particles.[48] Other researchers reported only 12% enhancement at similar particle concentrations.[10] More importantly, they also investigated variation in the thermal conductivity enhancement as a function of pH and found that increasing pH dramatically dampened any enhancements. Above pH 9, a 17 wt % (5 vol %) titania nanofluid had negligible enhancements in thermal conductivity, which is also consistent

with agglomeration related thermal conductivity enhancement mechanisms. Another possible reason for such reported discrepancies in thermal conductivity of nanofluids could be the variation in thermal conductivity reported for titania powders ($1.4-11.8$ Wm^{-1} K^{-1}). Overall, our experimental results on thermal conductivity are on the lower end but within the spread of the literature results. The surface grafting process demonstrated here does not directly affect the thermal conductivity of the nanoparticles but indirectly affects the thermal conductivity of suspensions by preventing particle agglomeration.

Electrochemical Activity of Pristine and Modified TiO$_2$. To test the surface activity and accessibility of ions to the surface of modified nanoparticles, we conducted cyclic voltammetry (CV) tests on pristine and surface-modified nanoparticles in the form of solid-casted electrodes. CVs of both TiO$_2$ and TiO$_2$-S (Figure 8) show the Ti (III)/Ti (IV) redox couple (reductive
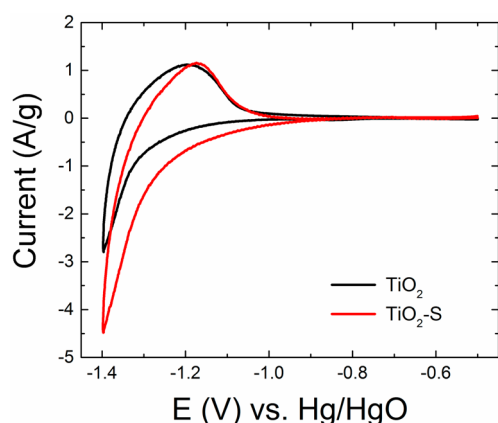

Figure 8. Cyclic voltammograms of pristine (TiO$_2$) and sulfonated titania (TiO$_2$-S) particles tested as a solid-casted electrode in 4 M KOH/1.5 M LiOH at scan rate of 5 mV/s.

peak at -1.3 V merged with onset of H$_2$ evolution and oxidative peak at -1.2 V). This redox couple has been associated with an accompanying lithiation/delithiation process in Li-ion containing electrolytes.[25] Although the position of redox peaks remains largely unchanged, the TiO$_2$-S material does exhibit a higher H$_2$ evolution current and smaller oxidative peak for the Ti (III)/Ti (IV) redox couple. Early onset of the hydrogen evolution reaction is most likely due to the acidic nature of the grafted moiety that could result in a local increase of [H$^+$], thereby shifting the concentration dependent H$_2$ evolution reaction potential. Comparison of the charge obtained by integration of the oxidative peaks for pristine and surface-modified titania revealed 22% reduction in the Ti (III)/Ti (IV) reaction due to the surface coating or competing H$_2$ evolution reaction. This suggests that at least 78% of the sulfonated titania surface is still accessible to the electrolyte, which can enable applications of formulated nanofluids in electrochemical and catalytic processes.

CONCLUSIONS

This study demonstrates a novel approach to formulating nanofluids with high solid nanoparticle loading, excellent colloidal stability, low viscosity, and good electrochemical response from the modified nanoparticles. A scalable one step procedure for the surface grafting of small organic molecules with negatively charged sulfonate groups onto the surface of titania nanoparticles is demonstrated. These grafted moieties comprise <3 wt % of the nanopowder weight and correspond to an

approximate monolayer coverage at the nanoparticle surface. Highly stable dispersions with up to 50 wt % of surface-modified TiO$_2$ particles in aqueous electrolytes (pH 11) were successfully obtained, which is 2.5 times higher than that achievable with pristine nanoparticles. It was demonstrated that the surface treatment minimizes particle agglomeration in electrolytes, providing small increases in viscosity (4.33 cP at 50 wt % in TiO$_2$-S nanofluids vs 15 cP at 20 wt % in pristine TiO$_2$ nanofluids, room temperature). Thermal conductivity measurements showed no effect on the surface modification at particle concentrations below the agglomeration threshold (e.g., 10 wt %). However, surface groups indirectly affect thermal conductivity of nanofluids at higher particle concentrations by preventing agglomeration of nanoparticles, which would otherwise provide additional pathways to heat conduction than that predicted by the effective medium theory. Electrochemical testing via cyclic voltammetry revealed two phenomena on surface-modified nanoparticles: early onset of H$_2$ evolution, most likely due to the acidic nature of the surface graft, resulting in the localized accumulation of [H$^+$] and partially suppressed (22% less than in pristine TiO$_2$) electrochemical response for the Ti (III)/Ti (IV) reaction, which could be due to the blockage of active sites by the graft or due to a competing H$_2$ evolution reaction. Nonetheless, 78% of the particle surface is accessible for redox processes.

We have demonstrated that the proposed surface modification technique meets the requirements for achieving nanofluids with desired properties: high particle loading, low viscosity, and high colloidal stability while simultaneously retaining thermal conductivity and electrochemical activity of the nanoparticles. Because of its simplicity and use of relatively mild reagents, the proposed surface treatment procedure can be easily scaled up to produce large quantities of modified nanoparticles. Future efforts will be directed at electrochemical testing of the nanofluids with high particle loadings as suspension electrodes or nano-electrofuels[8] for flow battery applications and further optimization of the surface coating to maximize electrochemical performance.

ASSOCIATED CONTENT

Ⓢ Supporting Information

The Supporting Information is available free of charge on the ACS Publications website at DOI: 10.1021/acsami.5b05864.

> Conversion of weight (wt %) to volume (vol %) fraction for titania nanoparticles, XRD and SEM analysis of titania nanoparticles of various sizes, evaluation of viscosity for nanofluids with different particle sizes of pristine TiO$_2$ anatase nanoparticles, estimation for surface coverage of titania nanoparticles with grafting agent, and shear rate dependence of viscosity (PDF)

AUTHOR INFORMATION

Corresponding Author
*E-mail: ssen@anl.gov.

Author Contributions
The manuscript was written by S.S. and E.V.T through contributions of all authors. All authors have given approval to the final version of the manuscript.

Notes
The authors declare no competing financial interest.

■ REFERENCES

(1) Taylor, R.; Coulombe, S.; Otanicar, T.; Phelan, P.; Gunawan, A.; Lv, W.; Rosengarten, G.; Prasher, R.; Tyagi, H. Small Particles, Big Impacts: A Review of the Diverse Applications of Nanofluids. *J. Appl. Phys.* **2013**, *113* (1), 011301−011319.

(2) Wong, K. V.; De Leon, O. Applications of Nanofluids: Current and Future. *Adv. Mech. Eng.* **2010**, *2010*, 1−11.

(3) Philip, J.; Shima, P. D. Thermal Properties of Nanofluids. *Adv. Colloid Interface Sci.* **2012**, *183−184* (0), 30−45.

(4) Yu, W.; France, D. M.; Singh, D.; Timofeeva, E. V.; Smith, D. S.; Routbort, J. L. Mechanisms and Models of Effective Thermal Conductivities of Nanofluids. *J. Nanosci. Nanotechnol.* **2010**, *10* (8), 4824−4849.

(5) Choi, S. U. S. Nanofluids: From Vision to Reality Through Research. *J. Heat Transfer* **2009**, *131* (3), 033106−033106.

(6) Cingarapu, S.; Singh, D.; Timofeeva, E. V.; Moravek, M. R. Nanofluids with Encapsulated Tin Nanoparticles for Advanced Heat Transfer and Thermal Energy Storage. *Int. J. Energy Res.* **2014**, *38* (1), 51−59.

(7) Khullar, V.; Tyagi, H.; Phelan, P. E.; Otanicar, T. P.; Singh, H.; Taylor, R. A. Solar Energy Harvesting Using Nanofluids-Based Concentrating Solar Collector. *J. Nanotechnol. Eng. Med.* **2012**, *3* (3), 031003−031003.

(8) Timofeeva, E. V.; Katsoudas, J. P. ; Segre, C. U.; Singh, D. Rechargeable Nanofluid Electrodes for High Energy Density Flow Battery. *Cleantech*, **2013**; Chapter 9, Energy Storage, pp 363−366.

(9) Chen, H.; Ding, Y.; He, Y.; Tan, C. Rheological Behaviour of Ethylene Glycol Based Titania Nanofluids. *Chem. Phys. Lett.* **2007**, *444* (4−6), 333−337.

(10) Ismay, M. J. L.; Doroodchi, E.; Moghtaderi, B. Effects of Colloidal Properties on Sensible Heat Transfer in Water-Based Titania Nanofluids. *Chem. Eng. Res. Des.* **2013**, *91* (3), 426−436.

(11) Joni, I. M.; Ogi, T.; Iwaki, T.; Okuyama, K. Synthesis of a Colorless Suspension of TiO_2 Nanoparticles by Nitrogen Doping and the Bead-Mill Dispersion Process. *Ind. Eng. Chem. Res.* **2013**, *52* (2), 547−555.

(12) Timofeeva, E. V.; Routbort, J. L.; Singh, D. Particle Shape Effects on Thermophysical Properties of Alumina Nanofluids. *J. Appl. Phys.* **2009**, *106* (1), 0143041−01430410.

(13) Utomo, A. T.; Poth, H.; Robbins, P. T.; Pacek, A. W. Experimental and Theoretical Studies of Thermal Conductivity, Viscosity and Heat Transfer Coefficient of Titania and Alumina Nanofluids. *Int. J. Heat Mass Transfer* **2012**, *55* (25−26), 7772−7781.

(14) Timofeeva, E. V.; Moravek, M. R.; Singh, D. Improving the Heat Transfer Efficiency of Synthetic Oil with Silica Nanoparticles. *J. Colloid Interface Sci.* **2011**, *364* (1), 71−79.

(15) Timofeeva, E. V.; Yu, W.; France, D. M.; Singh, D.; Routbort, J. L. Base Fluid and Temperature Effects on the Heat Transfer Characteristics of SiC in Ethylene Glycol/H_2O and H_2O Nanofluids. *J. Appl. Phys.* **2011**, *109* (1), 0149141−0149145.

(16) Shima, P. D.; Philip, J.; Raj, B. Synthesis of Aqueous and Nonaqueous Iron Oxide Nanofluids and Study of Temperature Dependence on Thermal Conductivity and Viscosity. *J. Phys. Chem. C* **2010**, *114* (44), 18825−18833.

(17) Moreira, L.; Carvalho, E. A.; Bell, M. J. V.; Anjos, V.; Sant'Ana, A. C.; Alves, A.; Fragneaud, B.; Sena, L. A.; Archanjo, B. S.; Achete, C. A. Thermo-optical Properties of Silver and Gold Nanofluids. *J. Therm. Anal. Calorim.* **2013**, *114* (2), 557−564.

(18) Yu, W.; Timofeeva, E. V.; Singh, D.; France, D. M.; Smith, R. K. Investigations of Heat Transfer of Copper-in-Therminol 59 Nanofluids. *Int. J. Heat Mass Transfer* **2013**, *64* (0), 1196−1204.

(19) Sinha, K.; Kavlicoglu, B.; Liu, Y.; Gordaninejad, F.; Graeve, O. A. A Comparative Study of Thermal Behavior of Iron and Copper Nanofluids. *J. Appl. Phys.* **2009**, *106* (6), 0643071−0643077.

(20) Halelfadl, S.; Maré, T.; Estellé, P. Efficiency of Carbon Nanotubes Water Based Nanofluids as Coolants. *Exp. Therm. Fluid Sci.* **2014**, *53* (0), 104−110.

(21) Buongiorno, J.; Venerus, D. C.; Prabhat, N.; McKrell, T.; Townsend, J.; Christianson, R.; Tolmachev, Y. V.; Keblinski, P.; Hu, L.-w.; Alvarado, J. L.; Bang, I. C.; Bishnoi, S. W.; Bonetti, M.; Botz, F.; Cecere, A.; Chang, Y.; Chen, G.; Chen, H.; Chung, S. J.; Chyu, M. K.; Das, S. K.; Di Paola, R.; Ding, Y.; Dubois, F.; Dzido, G.; Eapen, J.; Escher, W.; Funfschilling, D.; Galand, Q.; Gao, J.; Gharagozloo, P. E.; Goodson, K. E.; Gutierrez, J. G.; Hong, H.; Horton, M.; Hwang, K. S.; Iorio, C. S.; Jang, S. P.; Jarzebski, A. B.; Jiang, Y.; Jin, L.; Kabelac, S.; Kamath, A.; Kedzierski, M. A.; Kieng, L. G.; Kim, C.; Kim, J.-H.; Kim, S.; Lee, S. H.; Leong, K. C.; Manna, I.; Michel, B.; Ni, R.; Patel, H. E.; Philip, J.; Poulikakos, D.; Reynaud, C.; Savino, R.; Singh, P. K.; Song, P.; Sundararajan, T.; Timofeeva, E.; Tritcak, T.; Turanov, A. N.; Van Vaerenbergh, S.; Wen, D.; Witharana, S.; Yang, C.; Yeh, W.-H.; Zhao, X.-Z.; Zhou, S.-Q. A Benchmark Study on the Thermal Conductivity of Nanofluids. *J. Appl. Phys.* **2009**, *106* (9), 0943121−09431214.

(22) Kleinstreuer, C.; Feng, Y. Experimental and Theoretical Studies of Nanofluid Thermal Conductivity Enhancement: A Review. *Nanoscale Res. Lett.* **2011**, *6* (229), 1−13.

(23) Timofeeva, E. V.; Yu, W.; France, D. M.; Singh, D.; Routbort, J. L. Nanofluids for Heat Transfer: An Engineering Approach. *Nanoscale Res. Lett.* **2011**, *6* (182), 1−7.

(24) Hadjiivanov, K. I.; Klissurski, D. G. Surface Chemistry of Titania (Anatase) and Titania-Supported Catalysts. *Chem. Soc. Rev.* **1996**, *25* (1), 61−69.

(25) Liu, S.; Pan, G. L.; Yan, N. F.; Gao, X. P. Aqueous TiO_2/Ni(OH)_2 Rechargeable Battery with a High Voltage Based on Proton and Lithium Insertion/Extraction Reactions. *Energy Environ. Sci.* **2010**, *3* (11), 1732−1735.

(26) Timofeeva, E. V.; Smith, D. S.; Yu, W.; France, D. M.; Singh, D.; Routbort, J. L. Particle Size and Interfacial Effects on Thermo-physical and Heat Transfer Characteristics of Water-based α-SiC Nanofluids. *Nanotechnology* **2010**, *21* (21), 215703, 1−10.

(27) Prasher, R.; Evans, W.; Meakin, P.; Fish, J.; Phelan, P.; Keblinski, P. Effect of Aggregation on Thermal Conduction in Colloidal Nanofluids. *Appl. Phys. Lett.* **2006**, *89* (14), 143119, 1−3.

(28) Gharagozloo, P. E.; Goodson, K. E. Aggregate Fractal Dimensions and Thermal Conduction in Nanofluids. *J. Appl. Phys.* **2010**, *108* (7), 074309 1−7.

(29) Hidehiro, K.; Motoyuki, I. Surface Modification and Characterization for Dispersion Stability of Inorganic Nanometer-Scaled Particles in Liquid Media. *Sci. Technol. Adv. Mater.* **2010**, *11* (4), 044304.

(30) Zhao, J.-F.; Luo, Z.-Y.; Ni, M.-J.; Cen, K.-F. Dependence of Nanofluid Viscosity on Particle Size and pH Value. *Chin. Phys. Lett.* **2009**, *26* (6), 066202, 1−3.

(31) Ghadimi, A.; Saidur, R.; Metselaar, H. S. C. A Review of Nanofluid Stability Properties and Characterization in Stationary Conditions. *Int. J. Heat Mass Transfer* **2011**, *54* (17−18), 4051−4068.

(32) Farrokhi-rad, M.; Ghorbani, M. Stability of Titania Nano-particles in Different Alcohols. *Ceram. Int.* **2012**, *38* (5), 3893−3900.

(33) Ghadimi, A.; Metselaar, I. H. The Influence of Surfactant and Ultrasonic Processing on Improvement of Stability, Thermal Conductivity and Viscosity of Titania Nanofluid. *Exp. Therm. Fluid Sci.* **2013**, *51* (0), 1−9.

(34) Penkavova, V.; Tihon, J.; Wein, O. Stability and Rheology of Dilute TiO_2-water Nanofluids. *Nanoscale Res. Lett.* **2011**, *6* (273), 1−7.

(35) He, Y.; Jin, Y.; Chen, H.; Ding, Y.; Cang, D.; Lu, H. Heat Transfer and Flow Behaviour of Aqueous Suspensions of TiO_2 Nanoparticles (nanofluids) Flowing Upward Through a Vertical Pipe. *Int. J. Heat Mass Transfer* **2007**, *50* (11−12), 2272−2281.

(36) Kim, S. H.; Choi, S. R.; Kim, D. Thermal Conductivity of Metal-Oxide Nanofluids: Particle Size Dependence and Effect of Laser Irradiation. *J. Heat Transfer* 2006, *129* (3), 298−307.

(37) Yoo, D.-H.; Hong, K. S.; Yang, H.-S. Study of Thermal Conductivity of Nanofluids for the Application of Heat Transfer Fluids. *Thermochim. Acta* 2007, *455* (1−2), 66−69.

(38) Tseng, A. A.; Bellerová, H.; Pohanka, M.; Raudensky, M. Effects of Titania Nanoparticles on Heat Transfer Performance of Spray Cooling with Full Cone Nozzle. *Appl. Therm. Eng.* 2014, *62* (1), 20−27.

(39) Ding, Y.; Chen, H.; He, Y.; Lapkin, A.; Yeganeh, M.; Šiller, L.; Butenko, Y. V. Forced Convective Heat Transfer of Nanofluids. *Adv. Powder Technol.* 2007, *18* (6), 813−824.

(40) Chen, H.; Yang, W.; He, Y.; Ding, Y.; Zhang, L.; Tan, C.; Lapkin, A. A.; Bavykin, D. V. Heat Transfer and Flow Behaviour of Aqueous Suspensions of Titanate Nanotubes (Nanofluids). *Powder Technol.* 2008, *183* (1), 63−72.

(41) Wang, X.-Q.; Mujumdar, A. S. Heat Transfer Characteristics of Nanofluids: A Review. *Int. J. Therm. Sci.* 2007, *46* (1), 1−19.

(42) Cabaleiro, D.; Nimo, J.; Pastoriza-Gallego, M. J.; Piñeiro, M. M.; Legido, J. L.; Lugo, L. Thermal Conductivity of Dry Anatase snd Rutile Nano-Powders snd Ethylene snd Propylene Glycol-Based TiO$_2$ Nanofluids. *J. Chem. Thermodyn.* 2015, *83* (0), 67−76.

(43) Hu, Y.; He, Y.; Wang, S.; Wang, Q.; Inaki Schlaberg, H. Experimental and Numerical Investigation on Natural Convection Heat Transfer of TiO$_2$−Water Nanofluids in a Square Enclosure. *J. Heat Transfer* 2014, *136* (2), 022502−022502.

(44) Longo, G. A.; Zilio, C. Experimental Measurement of Thermophysical Properties of Oxide−Water Nano-Fluids Down to Ice-Point. *Exp. Therm. Fluid Sci.* 2011, *35* (7), 1313−1324.

(45) Saleh, R.; Putra, N.; Wibowo, R. E.; Septiadi, W. N.; Prakoso, S. P. Titanium Dioxide Nanofluids for Heat Transfer Applications. *Exp. Therm. Fluid Sci.* 2014, *52* (0), 19−29.

(46) Turgut, A.; Tavman, I.; Chirtoc, M.; Schuchmann, H. P.; Sauter, C.; Tavman, S. Thermal Conductivity and Viscosity Measurements of Water-Based TiO$_2$ Nanofluids. *Int. J. Thermophys.* 2009, *30* (4), 1213−1226.

(47) Wang, Z. L.; Tang, D. W.; Liu, S.; Zheng, X. H.; Araki, N. Thermal-Conductivity and Thermal-Diffusivity Measurements of Nanofluids by 3ω Method and Mechanism Analysis of Heat Transport. *Int. J. Thermophys.* 2007, *28* (4), 1255−1268.

(48) Murshed, S. M. S.; Leong, K. C.; Yang, C. Enhanced Thermal Conductivity of TiO$_2$−Water Based Nanofluids. *Int. J. Therm. Sci.* 2005, *44* (4), 367−373.

(49) Fedele, L.; Colla, L.; Bobbo, S. Viscosity and Thermal Conductivity Measurements of Water-Based Nanofluids Containing Titanium Oxide Nanoparticles. *Int. J. Refrig.* 2012, *35* (5), 1359−1366.

(50) Tseng, W. J.; Lin, K.-C. Rheology And Colloidal Structure of Aqueous TiO$_2$ Nanoparticle Suspensions. *Mater. Sci. Eng., A* 2003, *355* (1−2), 186−192.

(51) Chandler, H. D. Flow Mechanisms and Rheology of Dense Aqueous Suspensions of Titanium (IV) Oxide. *Rheol. Acta* 2010, *49* (4), 349−357.

(52) Gómez-Merino, A. I.; Rubio-Hernández, F. J.; Velázquez-Navarro, J. F.; Aguiar, J.; Jiménez-Agredano, C. Study of The Aggregation State of Anatase Water Nanofluids Using Rheological and DLS Methods. *Ceram. Int.* 2014, *40* (9, Part A), 14045−14050.

(53) Yang, H.-G.; Li, C.-Z.; Gu, H.-C.; Fang, T.-N. Rheological Behavior of Titanium Dioxide Suspensions. *J. Colloid Interface Sci.* 2001, *236* (1), 96−103.

(54) Kango, S.; Kalia, S.; Celli, A.; Njuguna, J.; Habibi, Y.; Kumar, R. Surface Modification of Inorganic Nanoparticles for Development of Organic−Inorganic Nanocomposites—A Review. *Prog. Polym. Sci.* 2013, *38* (8), 1232−1261.

(55) Neouze, M.-A.; Schubert, U. Surface Modification and Functionalization of Metal and Metal Oxide Nanoparticles by Organic Ligands. *Monatsh. Chem.* 2008, *139* (3), 183−195.

(56) Baraton, M.-I. Surface Chemistry and Functionalization of Semiconducting Nanosized Particles. In *Nanostructures: Synthesis, Functional Properties and Applications*; Tsakalakos, T., Ovid'ko, I.,

Vasudevan, A., Eds.; Springer: Netherlands, 2003; Chapter 24, pp 427−440.

(57) Bloemen, M.; Brullot, W.; Luong, T.; Geukens, N.; Gils, A.; Verbiest, T. Improved Functionalization of Oleic Acid-Coated Iron Oxide Nanoparticles for Biomedical Applications. *J. Nanopart. Res.* 2012, *14* (9), 1−10.

(58) Atghia, S.; Beigbaghlou, S. Nanocrystalline Titania-Based Sulfonic Acid (TiO$_2$-Pr-SO$_3$H) as a New, Highly Efficient, and Recyclable Solid Acid Catalyst For Preparation of Quinoxaline Derivatives. *J. Nanostruct. Chem.* 2013, *3* (1), 1−8.

(59) Atghia, S. V.; Sarvi Beigbaghlou, S. Nanocrystalline Titania-Based Sulfonic Acid (TiO$_2$-Pr-SO$_3$H) as a New, Highly Efficient And Recyclable Solid Acid Catalyst For The N-Boc Protection Of Amines At Room Temperature. *J. Organomet. Chem.* 2013, *745−746* (0), 42−49.

(60) Rahmani, S.; Amoozadeh, A.; Kolvari, E. Nano Titania-Supported Sulfonic Acid: An Efficient and Reusable Catalyst for a Range of Organic Reactions Under Solvent Free Conditions. *Catal. Commun.* 2014, *56* (0), 184−188.

(61) Ma, Z.; Yue, Y.; Deng, X.; Gao, Z. Nanosized Anatase TiO$_2$ as Precursor for Preparation of Sulfated Titania Catalysts. *J. Mol. Catal. A: Chem.* 2002, *178* (1−2), 97−104.

(62) Ropero-Vega, J. L.; Aldana-Pérez, A.; Gómez, R.; Niño-Gómez, M. E. Sulfated Titania [TiO$_2$/SO$_4^{2-}$]: A Very Active Solid Acid Catalyst for the Esterification of Free Fatty Acids with Ethanol. *Appl. Catal., A* 2010, *379* (1−2), 24−29.

(63) Samantaray, S. K.; Mishra, T.; Parida, K. M. Studies on Anion Promoted Titania: 2: Preparation, Characterisation and Catalytic Activity Towards Aromatic Alkylation Over Sulfated Titania. *J. Mol. Catal. A: Chem.* 2000, *156* (1−2), 267−274.

(64) Sunajadevi, K. R.; Sugunan, S. Sulfated Titania Mediated Regioselective Nitration of Phenol in Solid State. *Catal. Commun.* 2005, *6* (9), 611−616.

(65) Sun, T.; Teja, A. S. Density, Viscosity, and Thermal Conductivity of Aqueous Ethylene, Diethylene, and Triethylene Glycol Mixtures between 290 and 450 K. *J. Chem. Eng. Data* 2003, *48* (1), 198−202.

(66) Weirich, T. E.; Winterer, M.; Seifried, S.; Mayer, J. Structure of Nanocrystalline Anatase Solved and Refined from Electron Powder Data. *Acta Crystallogr., Sect. A: Found. Crystallogr.* 2002, *58* (4), 308−315.

(67) Mikulášek, P.; Wakeman, R. J.; Marchant, J. Q. The Influence of pH and Temperature on the Rheology and Stability of Aqueous Titanium Dioxide Dispersions. *Chem. Eng. J. (Amsterdam, Neth.)* 1997, *67* (2), 97−102.

(68) Using The Krieger−Dougherty Model to Predict Suspension Viscosity. Technical Note, version 5, Malvern Instruments. http://www.malvern.com/.

(69) Landau, L. D.; Lifshitz, E. M. Electrodynamika Sploshnykh Sred [Electrodynamics of Continuous Media], 27, Nauka: Moscow, 1992.

(70) Feng, X.; Huang, X.; Wang, X. Thermal Conductivity and Secondary Porosity of Single Anatase TiO$_2$ Nanowire. *Nanotechnology* 2012, *23*, 185701−185713.